Regular Article

Multistable systems with nested hidden and self-excited double scroll attractors

R. J. Escalante-González[1,a] and Eric Campos[2,b]

[1] Electrical, Electronic and Mechatronics Department, Technological Institute of San Luis Potosí, Tecnológico avenue, Soledad de Graciano Sànchez, 78437 San Luis Potosí, Mexico
[2] Division of Control and Dynamical Systems, Institute for Scientific and Technological Research of San Luis Potosí, Camino a la Presa San José 2055, Lomas 4 Sección, 78216 San Luis Potosí, S.L.P., Mexico

Abstract Systems with multiscroll attractors have been studied extensively in recent decades. Some efforts have focused on understanding the mechanisms that generate complex dynamics in relatively simple systems. The chaotic properties of these systems have been found useful in cryptographic techniques. Recently, hidden chaotic attractors have raised interest in cryptographic algorithms due to the additional complexity they provide. Although several hidden chaotic attractors have been reported, the variety of mechanisms involved in the appearance of hidden attractors in multistable systems is not fully understood. Here we report an approach to generate multistable systems with nested hidden attractors. The idea behind the construction is to use a nonlinear function to produce coexisting self-excited attractors at specific locations. So, a hidden attractor emerges for each pair of self-excited attractors, each pair of these hidden attractors leads to the appearance of a larger hidden attractor. In this way, hidden nested attractors appear depending on the number of self-excited attractors. Therefore, the systems produced with the approach could possibly be used in a cryptographic algorithm. The new dynamical system to generate nested attractors starts by selecting three parameters which are related to the oscillatory behavior and appear in the linear part (matrix A) of the system equations. Then, using the proposed simplest system description, two parameters, which are related to the location of the equilibria, are adjusted in order to generate a bistable behavior with two self-excited attractors. Each of these self-excited attractors is generated by a pair of equilibrium points. Thus the two self-excited attractors emerge when the relationship between the separation of the two pairs of equilibria and the separation by pairs of equilibria is large enough, which is controlled by two parameters. The bistable behavior is found by choosing the appropriate parameters of the matrix A. Once the bistable behavior has been verified, the found parameters are used in the appropriate proposed description of the system for the desired number of attractors. A particular case with fifteen attractors is introduced.

1 Introduction

According to [1], we can find two classes of attractors in a system, those classical attractors self-excited by their unstable equilibria whose basin of attraction intersects with an open neighborhood of equilibria called *self-excited attractors*, and those whose basin of attraction does not contain neighborhoods of equilibria called *hidden attractors*. The localization of hidden attractors is generally more difficult than in the case of self-excited attractors. An analytical-numerical algorithm was suggested in [1] for the localization of hidden attractors of Chua's circuit.

Recently, the use of hidden chaotic attractors instead of self-excited attractors in cryptographic algorithms

has been shown to increase security [2]. Some systems with hidden attractors have been studied in [3–15], however, most of the mechanisms that lead to the appearance of hidden attractors in the wide variety of classes of systems remain unexplored.

The concept of multistability in a system is usually related to the existence of two or more attractors. If at least one of these is a hidden attractor, it adds additional complexity since its location is not as simple as in the case of a self-excited attractor.

In [16] a study is presented on the widening of the basins of attraction in multistable piecewise linear systems. In this work, a system with two double-scroll self-excited attractors and one double-scroll hidden attractor is reported. The hidden attractor resembles a larger double-scroll attractor in that the self-excited attractors act similarly to the equilibria in the center of the scrolls of a self-excited double-scroll attractor. This

ᵃ e-mail: rodolfo.eg@slp.tecnm.mx (corresponding author)

ᵇ e-mail: eric.campos@ipicyt.edu.mx

behavior was studied in [17] for a class of piecewise linear systems that lead to the construction of multistable systems with hidden grid attractors. In the center of each scroll of this grid attractor is a self-excited attractor. Based on the previous results and with the objective of increasing the complexity of multistable systems, we propose an approach which allows the generation of $2^m - 1$ nested hidden attractors, with $m \in \mathbb{N}$. The approach allows the construction of complicated multistable systems where the shape of both, self-excited and hidden attractors can be modified. With this nested arrangement, more than one attractor can be found in the center of a scroll of another attractor, which leads to more complex attraction basins. Since the approach allows the construction of complicated multistable systems with any number of hidden attractors, a possible application in cryptography is expected.

The structure of this work is as follows: In Sect. 2, the approach to generate nested hidden attractors is introduced. In Sect. 3, two particular cases are presented, one with two self excited attractors and one hidden attractor and another with fifteen attractors. In Sect. 4 some conclusions are given.

2 Approach description

In order to introduce the approach let us define $P = \{P_1, \ldots, P_\eta\}$, with $\eta > 1$ and $\eta \in \mathbb{N}$, as a finite partition of $X \subset \mathbb{R}^3$. Now let $T : X \to X$, with $X \subset \mathbb{R}^3$, be a piecewise linear dynamical system whose dynamics is given by a family of sub-systems of the form

$$\dot{\mathbf{x}} = A\mathbf{x} + f(\mathbf{x})B, \qquad (1)$$

where $\mathbf{x} = (x_1, x_2, x_3)^{\mathrm{T}} \in \mathbb{R}^3$ is the state vector, $A = \{\alpha_{ij}\} \in \mathbb{R}^{3 \times 3}$ is a linear operator, $B = (\beta_1, \beta_2, \beta_3)^{\mathrm{T}}$ is a constant vector, and f is a functional. The vector $f(\mathbf{x})B$ is a constant vector in each atom P_i such that the equilibria is given by $\mathbf{x}^*_{\mathrm{eq}_i} = (x^*_{1_{\mathrm{eq}_i}}, x^*_{2_{\mathrm{eq}_i}}, x^*_{3_{\mathrm{eq}_i}})^{\mathrm{T}} = -f(\mathbf{x})A^{-1}B \in P_i$, with $i = 1, \ldots, \eta$.

The matrix of the linear operator A is defined as follows:

$$A = \begin{pmatrix} \frac{a}{3} + \frac{2c}{3} & b & \frac{2c}{3} - \frac{2a}{3} \\ -\frac{b}{3} & a & \frac{2b}{3} \\ \frac{c}{3} - \frac{a}{3} & -b & \frac{2a}{3} + \frac{c}{3} \end{pmatrix}, \qquad (2)$$

where $a, b \in \mathbb{R}^+$ and $c \in \mathbb{R}^-$. The complexification of A, $A^{\mathbb{C}}$ has the eigenvalues $\lambda_1 = a + ib$, $\lambda_2 = a - ib$ and $\lambda_3 = c$. Then the equilibrium point in each element of the partition P is a saddle point whose unstable manifold is $W^U_{\mathbf{x}^*_{\mathrm{eq}_i}} = \{(\mathbf{x} + \mathbf{x}^*_{\mathrm{eq}_i}) \in \mathbb{R}^3 : \mathbf{x} \in \mathrm{span}\{v_1, v_2\}\}$ where $v_1 = (1\ 0\ \frac{1}{2})^{\mathrm{T}}$ and $v_2 = (0\ -1\ 0)^{\mathrm{T}}$. The stable manifold is $W^S_{\mathbf{x}^*_{\mathrm{eq}_i}} = \{(\mathbf{x} + \mathbf{x}^*_{\mathrm{eq}_i}) \in \mathbb{R}^3 : \mathbf{x} \in \mathrm{span}\{v_3\}\}$ where $v_3 = (-1\ 0\ 1)^{\mathrm{T}}$.

The selection of this matrix A is based on the idea that each equilibrium point $\mathbf{x}^*_{\mathrm{eq}_i}$ is a saddle equilib-

rium point, and furthermore, if two equilibria $\mathbf{x}^*_{\mathrm{eq}_1}$ and $\mathbf{x}^*_{\mathrm{eq}_2}$ are symmetrically separated along axis x_1 from a surface $\Sigma = \{\mathbf{x} \in \mathbb{R}^3 : x_1 = \rho, \rho \in \mathbb{R}\}$ then $W^U_{\mathbf{x}^*_{\mathrm{eq}_1}} \cap W^S_{\mathbf{x}^*_{\mathrm{eq}_2}} \cap \Sigma = \emptyset$ and $W^S_{\mathbf{x}^*_{eq_1}} \cap W^U_{\mathbf{x}^*_{\mathrm{eq}_2}} \cap \Sigma = \emptyset$. This condition is related to the existence of a hidden attractor and was observed before in [17].

The constant vector $B \in \mathbb{R}^3$ is given by:

$$B = \begin{pmatrix} -\frac{a}{3} - \frac{2c}{3} \\ \frac{b}{3} \\ \frac{a}{3} - \frac{c}{3} \end{pmatrix}, \qquad (3)$$

The functional $f(\mathbf{x})$ is:

$$f(\mathbf{x}) = \alpha u \left(2 \left(x_1 - \sum_{i=1}^{m} w_i \right) - x_3,\ x_3 \right) + \sum_{i=1}^{m} w_i, \quad (4)$$

where $\alpha \in \mathbb{R}$, $m \in \mathbb{N}$, and w_i are defined as follows

$$w_0 = 0, \qquad (5)$$

$$w_i = \gamma^{m+1-i} u \left(x_1 - \sum_{j=0}^{i-1} w_j, x_3 \right), \quad \text{for } i = 1, \ldots, m,$$

$$\text{and } m \geq 1, \qquad (6)$$

where $\gamma \in \mathbb{R}$, $u(x_1, x_3)$ is a binary function with two arguments, x_1 and x_3, that function values are 1 or -1 depending on its arguments x_1 and x_3. Note that for $x_1 = 0$ can be mapped to 1 or -1 depending on the value of x_3. The function $u(x_1, x_3)$ is defined as follows:

$$u(x, z) = \begin{cases} 1, & \text{if } x > 0 \text{ and } z \geq 0; \\ -1, & \text{if } x \leq 0 \text{ and } z \geq 0; \\ 1, & \text{if } x \geq 0 \text{ and } z < 0; \\ -1, & \text{if } x < 0 \text{ and } z < 0. \end{cases} \qquad (7)$$

The functional $f(\mathbf{x})$ is responsible for the location of the equilibria. In order to analyze it let us rewrite it as $f(\mathbf{x}) = f_1 + f_2$. The functional $f(\mathbf{x})$ acts on a partition P which is determined by dividing the atoms of a partition G defined by the function f_2. Therefore, first, we consider the function $f_2 = \sum_{i=1}^{m} w_i$, for $m = 1$ it takes the form:

$$f_2 = w_1 = \gamma u(x_1, x_3), \qquad (8)$$

which generates a partition $G = \{G_1, G_2\}$ with the switching surface $\{\mathbf{x} \in \mathbb{R}^3 : x_1 = 0\}$ such that for $\mathbf{x}$ in G_1, we have $f_2 = -\gamma$, and for $\mathbf{x}$ in G_2, $f_2 = \gamma$. The partition P is given by dividing the atoms G_1 and G_2 according to the function f_1. The way how the atoms G_1 and G_2 are divided is shown below. Now, let us consider $m = 2$ then

$$w_1 = \gamma^2 u(x_1, x_3), \qquad (9)$$
$$w_2 = \gamma u(x_1 - \gamma^2 u(x_1, x_3), x_3), \qquad (10)$$

Eur. Phys. J. Spec. Top. (2022) 231:351–357

353

$$f_2 = \gamma u(x_1 - \gamma^2 u(x_1, x_3), x_3) + \gamma^2 u(x_1, x_3). \quad (11)$$

This can be interpreted by parts: first, w_1 generates a partition $G = \{G_1, G_2\}$ with the switching surface $\{\mathbf{x} \in \mathbb{R}^3 : x_1 = 0\}$ such that for $\mathbf{x}$ in G_1, we have $w_1 = -\gamma^2$ and for $\mathbf{x}$ in G_2, $w_1 = \gamma^2$. Then, w_2 generates a partition in G_1 as follows $G_1 = \{G_{11}, G_{12}\}$ with the switching surface $\{\mathbf{x} \in \mathbb{R}^3 : x_1 = w_1 = -\gamma^2\}$. Also, w_2 generates a partition in G_2 as follows $G_2 = \{G_{21}, G_{22}\}$ with the switching surface $\{\mathbf{x} \in \mathbb{R}^3 : x_1 = w_1 = \gamma^2\}$. Thus, the location of the switching surfaces along the x_1 axis is $x_1 \in \{-\gamma^2, 0, \gamma^2\}$. Since $f_2 = w_1 + w_2$ it follows that:

$$f_2 = \begin{cases} -\gamma^2 - \gamma & \text{if } \mathbf{x} \in G_{11}; \\ \gamma^2 + \gamma & \text{if } \mathbf{x} \in G_{12}; \\ \gamma^2 - \gamma & \text{if } \mathbf{x} \in G_{21}; \\ \gamma^2 + \gamma & \text{if } \mathbf{x} \in G_{22}. \end{cases} \quad (12)$$

If $m = 3$ then the elements of the partition are doubled as $G = \{G_{111}, G_{112}, G_{121}, G_{122}, \ldots, G_{221}, G_{222}\}$ and since $f_2 = w_1 + w_2 + w_3$:

$$f_2 = \begin{cases} -\gamma^3 - \gamma^2 - \gamma & \text{if } \mathbf{x} \in G_{111}; \\ -\gamma^3 - \gamma^2 + \gamma & \text{if } \mathbf{x} \in G_{112}; \\ -\gamma^3 + \gamma^2 - \gamma & \text{if } \mathbf{x} \in G_{121}; \\ -\gamma^3 + \gamma^2 + \gamma & \text{if } \mathbf{x} \in G_{122}; \\ \gamma^3 - \gamma^2 - \gamma & \text{if } \mathbf{x} \in G_{211}; \\ \gamma^3 - \gamma^2 + \gamma & \text{if } \mathbf{x} \in G_{212}; \\ \gamma^3 + \gamma^2 - \gamma & \text{if } \mathbf{x} \in G_{221}; \\ \gamma^3 + \gamma^2 + \gamma & \text{if } \mathbf{x} \in G_{222}; \end{cases} \quad (13)$$

while the switching surfaces are located along the x_1 axis as $x_1 \in \{-\gamma^3 - \gamma^2, -\gamma^3 + \gamma^2, 0, \gamma^3 - \gamma^2, \gamma^3 + \gamma^2\}$.

Then, one way to see the function f_2 is that for each time that m changes to $m + 1$ the elements of the previous partition are doubled. The number of elements of the partition G is 2^m.

It is worth mentioning that each atom of the partition P contains an equilibrium point which is determined by the functional f. Also, the partition P is generated by dividing the atoms of the partition G, then the atoms of the partition P are twice of the atoms of the partition G. Furthermore, the functional f is designed to allow the generation of heteroclinic orbits between a pair of equilibria which are contained in the same atom of the partition G.

Now, let us analyze the term f_1 which can be rewritten as

$$\begin{aligned} f_1 &= \alpha u\left(2\left(x_1 - \sum_{i=1}^{m} w_i\right) - x_3, \ x_3\right) \\ &= \alpha u\left(2(x_1 - f_2) - x_3, \ x_3\right). \end{aligned} \quad (14)$$

Therefore, f_1 is basically the step function $u(x, z)$ with a scaling factor α. The arguments of $u(x_1, x_3)$ take this form to generate switching surfaces with the orientation required to generate the heteroclinic loops between

equilibria in adjacent atoms given by P_i and P_{i+1}, with $i = 1, 3, 5, \ldots, 2^{m+1} - 1$.

Thus f_1 generates a partition with two elements for each element of the partition generated by f_2. Then the final partition is $P = \{P_1, \ldots, P_{2^{m+1}}\}$. In each element of the partition G there is a switching surface of the form $\{\mathbf{x} \in \mathbb{R}^3, \epsilon \in \mathbb{R} : 2x_1 - x_3 = \epsilon\}$. Also, the number of equilibria is 2^{m+1} which under appropriate parameter values generates 2^m self-excited attractors. For each pair of self-excited attractors a hidden attractor could emerge as well as for two hidden attractors could emerge a new hidden attractor.

Then, for $m = 1$ there are two self-excited attractors and one hidden attractor, each time m is incremented the attractors (self-excited and hidden) are multiplied by two and a new hidden attractor can emerge. Thus, the total number of hidden attractors is $2^m - 1$ and the total number of self excited attractors is 2^m. The total number of coexisting attractors is then $2^m + 2^m - 1 = 2^{m+1} - 1$.

The equilibria is located along the x_1 axis depending on α, m and γ. The equilibria for $m \in \{1, 2, 3\}$ is shown in Table 1. Each self-excited attractor oscillates around a pair of equilibria $\mathbf{x}_{eq_k}^*$ and $\mathbf{x}_{eq_{k+1}}^*$, with $k = 1, 3, \ldots, 2^{m+1} - 1$.

3 Particular cases of nested hidden and self-excited double scroll attractors

To illustrate the approach, consider the simplest case for $m = 1$ along with $\alpha = 1$, $\gamma = 10$, the system presents three attractors, a hidden attractor and two self-excited attractors. In the Fig. 1, two self excited attractors are shown in red and a hidden attractor in blue. The double-scroll self-excited attractors are nested in each scroll of the hidden attractor.

Now in order to illustrate the approach with a more complex case, consider the values $m = 3$, $\alpha = 1$, $\gamma = 10$. The number of attractors is now fifteen, eight self-excited and seven hidden attractors. Projection of the attractors on the (x_1, x_2) plane are presented in the Fig. 2, the self-excited attractors are drawn in black. There are eight double-scroll self-excited attractors and the projection of one of them on the (x_1, x_2) plane is shown in Fig. 2a. A pair of double-scroll self-excited attractors are used to generate a double-scroll hidden attractor. Figure 2b shows the projection of a double-scroll hidden attractor in green which is generated by a pair of self-excited attractors in black. Therefore, the eight double-scroll self-excited attractors generate four double-scroll hidden attractors in green. Each scroll of the green hidden attractor has a self-excited attractor nested. Each pair of green hidden attractors generates a new hidden attractor. Figure 2c shows the projections of three hidden attractors on the (x_1, x_2) plane, the double-scroll hidden attractor in red is generated by two hidden attractors in green. Then, the four green attractors generate two red hidden attractors. Each scroll of

Table 1 Location of the equilibria along the x_1 axist depending on m, α and γ for $m \in [1,3]$

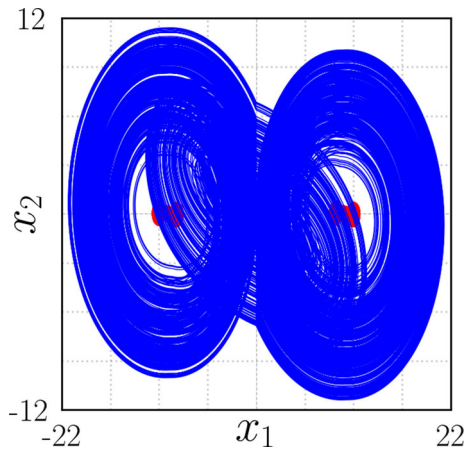| m	Location at x_1
$m = 1$	$-\gamma - \alpha, -\gamma + \alpha, \gamma - \alpha, \gamma + \alpha$
$m = 2$	$-\gamma^2 - \gamma - \alpha, -\gamma^2 - \gamma + \alpha, -\gamma^2 + \gamma - \alpha, -\gamma^2 + \gamma + \alpha,$
	$\gamma^2 - \gamma - \alpha, \gamma^2 - \gamma + \alpha, \gamma^2 + \gamma - \alpha, \gamma^2 + \gamma + \alpha$
$m = 3$	$-\gamma^3 + \gamma^2 - \gamma - \alpha, -\gamma^3 + \gamma^2 - \gamma + \alpha, -\gamma^3 + \gamma^2 + \gamma - \alpha, -\gamma^3 + \gamma^2 + \gamma + \alpha,$
	$-\gamma^3 - \gamma^2 - \gamma - \alpha, -\gamma^3 - \gamma^2 - \gamma + \alpha, -\gamma^3 - \gamma^2 + \gamma - \alpha, -\gamma^3 - \gamma^2 + \gamma + \alpha,$
	$\gamma^3 + \gamma^2 - \gamma - \alpha, \gamma^3 + \gamma^2 - \gamma + \alpha, \gamma^3 + \gamma^2 + \gamma - \alpha, \gamma^3 + \gamma^2 + \gamma + \alpha,$
	$\gamma^3 - \gamma^2 - \gamma - \alpha, \gamma^3 - \gamma^2 - \gamma + \alpha, \gamma^3 - \gamma^2 + \gamma - \alpha, \gamma^3 - \gamma^2 + \gamma + \alpha$

Fig. 1 Projection of the three attractors on the (x_1, x_2) plane: Two self-excited attractors (red) and a hidden attractor (blue) exhibited for $m = 1, \alpha = 1, \gamma = 10$

the red hidden attractor has a green hidden attractor nested. And so on, the two red hidden attractors generate a larger double-scroll hidden attractor which is drawn in blue in Fig. 2d. Therefore, each scroll of the blue hidden attractor has seven attractors nested, i.e. a red hidden attractor, two green hidden attractors, and four self-excited attractors.

The Lyapunov exponents have been calculated for the fifteen attractors with the Wolf's algorithm [18] using $\tanh(Nx_1)$ approximations, Kaplan–Yorke dimension was also calculated for all the attractors and is presented along the exponents in Table 2.

According to [19] the diameter of a set is defined as follows:

Definition 31 [19] If S is a nonempty subset of $\mathbb{R}^n$, then

$$d(S) = \sup \left\{ |x - y| : x, y \in S \right\},$$

is the *diameter* of S. If $d(S) < \infty$, S is bounded, if $d(S) = \infty$, S is unbounded.

Subsets of the basins of attraction at the plane $\{x \in \mathbb{R}^3 : x_3 = 0\}$ were numerically estimated for the fifteen attractors and they are shown in the Fig. 3. As shown in the Fig. 3 the basins of attraction of different coexisting attractors occur as disjoint sets in the phase space, this

is due to the nested geometry of the attractors. Consider for instance the hidden attractor shown in Fig. 2b in green, its basin of attraction "surround" four equilibrium points, however, the equilibria are not part of it, neither the two self-excited attractors in black. The basin of attraction of each self-excited attractor "surround the two equilibria" but it is also "surrounded" by the basin of attraction of the hidden attractor.

The diameters of the estimated subsets of the basins of attraction are also presented in Table 2.

4 Conclusions

In this work an approach for the generation of multiple hidden attractors is presented, the approach allows the modification of shape and number of attractors via some parameters. The proposed approach could be performed following three steps: First, parameters a, b and c related to the eigenvalues of $A^{\mathbb{C}}$ are selected. Second, parameters γ and α that produce a bistable behavior are found via simulation. In case these were not found, new parameters can be chosen in the first step. Third, the found parameters are used in the appropriate proposed description of the system for the correct value of m according to the desired number of attractors. The new system is then simulated in order to verify the expected behavior as well as perform the characterization of the attractors. The particular cases used to illustrate the construction suggests that the generated attractors, self-excited as well as hidden are indeed chaotic. Even when the approach uses self-excited attractors as a base for the generation of hidden attractors these could be replaced by hidden double scroll attractors as those reported in [14] which would lead to a system without equilibria. The approach could also lead to other designs that exhibit not only double scroll attractors but different number of scrolls or even nested hidden grid attractors. The generation of a multiscroll hidden attractor along several self-excited attractors could be controlled for the use in a multi-channel communication scheme or even in the generation of pseudo-random numbers. Also, it seems plausible the modification of the approach to generate a fractal like continuous system where the attractors present self-similarity.

Fig. 2 In (**a**–**c**) smaller portions of the projection of the attractors are shown. In (**a**) a double-scroll self-excited attractor of eight self-excited attractors produced by the proposed construction given by (1), (2), (3) and (4) with $a = 0.2$, $b = 5$, $c = -3$, $m = 3$, $\alpha = 1$ and $\gamma = 10$ projected on $x_1 - x_2$. In (**b**) a double-scroll hidden attractor contained two nested double-scroll self-excited attractors, **c** three hidden attractors and four self-excited attractors, and **d** fifteen attractors are shown, seven hidden attractors and eight self-excited attractors
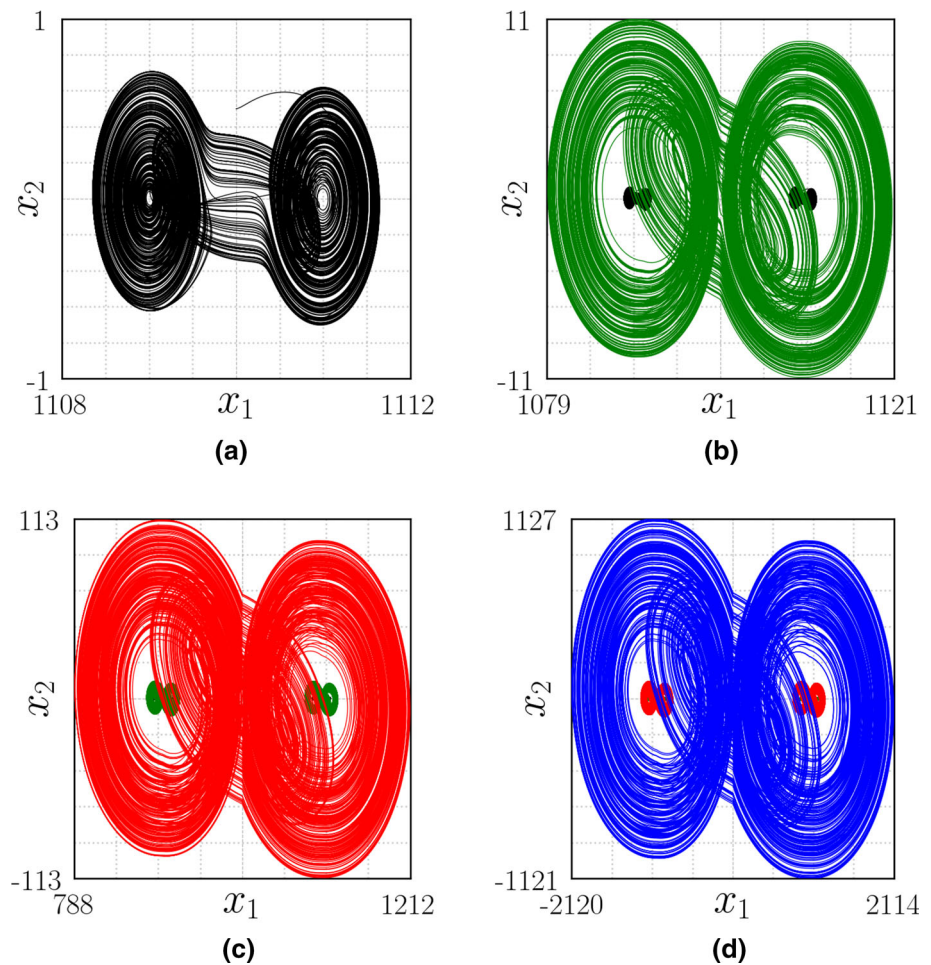

(a)

(b)

(c)

(d)

Table 2 Lyapunov exponents and Kaplan–Yorke dimension of the fifteen attractors produced by the proposed construction given by (1), (2), (3) and (4) with $a = 0.2$, $b = 5$, $c = -3$, $m = 3$, $\alpha = 1$ and $\gamma = 10$ as well as the diameter of the subset of the basin of attraction numerically

| Attractor | Center position | | Lyapunov | | Diameter |
	at x_1	$x(0)$	exponents	D_{KY}	$d(\cdot)$
1	-1110.0	$(-1110, 0.05, 0)^{\mathrm{T}}$	$0.343, -0.0, -2.745$	2.125	9.409
2	-1090.0	$(-1090, 0.05, 0)^{\mathrm{T}}$	$0.343, 0.0, -2.744$	2.125	9.409
3	-910.0	$(-910, 0.05, 0)^{\mathrm{T}}$	$0.348, -0.0, -2.744$	2.1268	9.409
4	-890.0	$(-890, 0.05, 0)^{\mathrm{T}}$	$0.347, 0.0, -2.744$	2.1265	9.409
5	890.0	$(890, 0.05, 0)^{\mathrm{T}}$	$0.35, -0.0, -2.745$	2.1275	9.409
6	910.0	$(910, 0.05, 0)^{\mathrm{T}}$	$0.346, 0.0, -2.743$	2.1261	9.409
7	1090.0	$(1090, 0.05, 0)^{\mathrm{T}}$	$0.346, 0.0, -2.741$	2.1262	9.409
8	1110.0	$(1110, 0.05, 0)^{\mathrm{T}}$	$0.341, 0.0, -2.739$	2.1245	9.409
9	-1100.0	$(-1100, 0.5, 0)^{\mathrm{T}}$	$0.306, -0.0, -2.509$	2.122	128.191
10	-900.0	$(-900, 0.5, 0)^{\mathrm{T}}$	$0.31, 0.0, -2.51$	2.1235	128.191
11	900.0	$(900, 0.5, 0)^{\mathrm{T}}$	$0.31, -0.0, -2.51$	2.1235	128.191
12	1100.0	$(1100, 0.5, 0)^{\mathrm{T}}$	$0.31, 0.0, -2.51$	2.1235	128.191
13	-1000.0	$(-1000, 5.0, 0)^{\mathrm{T}}$	$0.35, -0.02, -2.46$	2.1423	1302.459
14	1000.0	$(1000, 5.0, 0)^{\mathrm{T}}$	$0.35, -0.02, -2.46$	2.1423	1302.459
15	0.0	$(0, 50.0, 0)^{\mathrm{T}}$	$0.36, -0.03, -2.43$	2.1481	13201.515
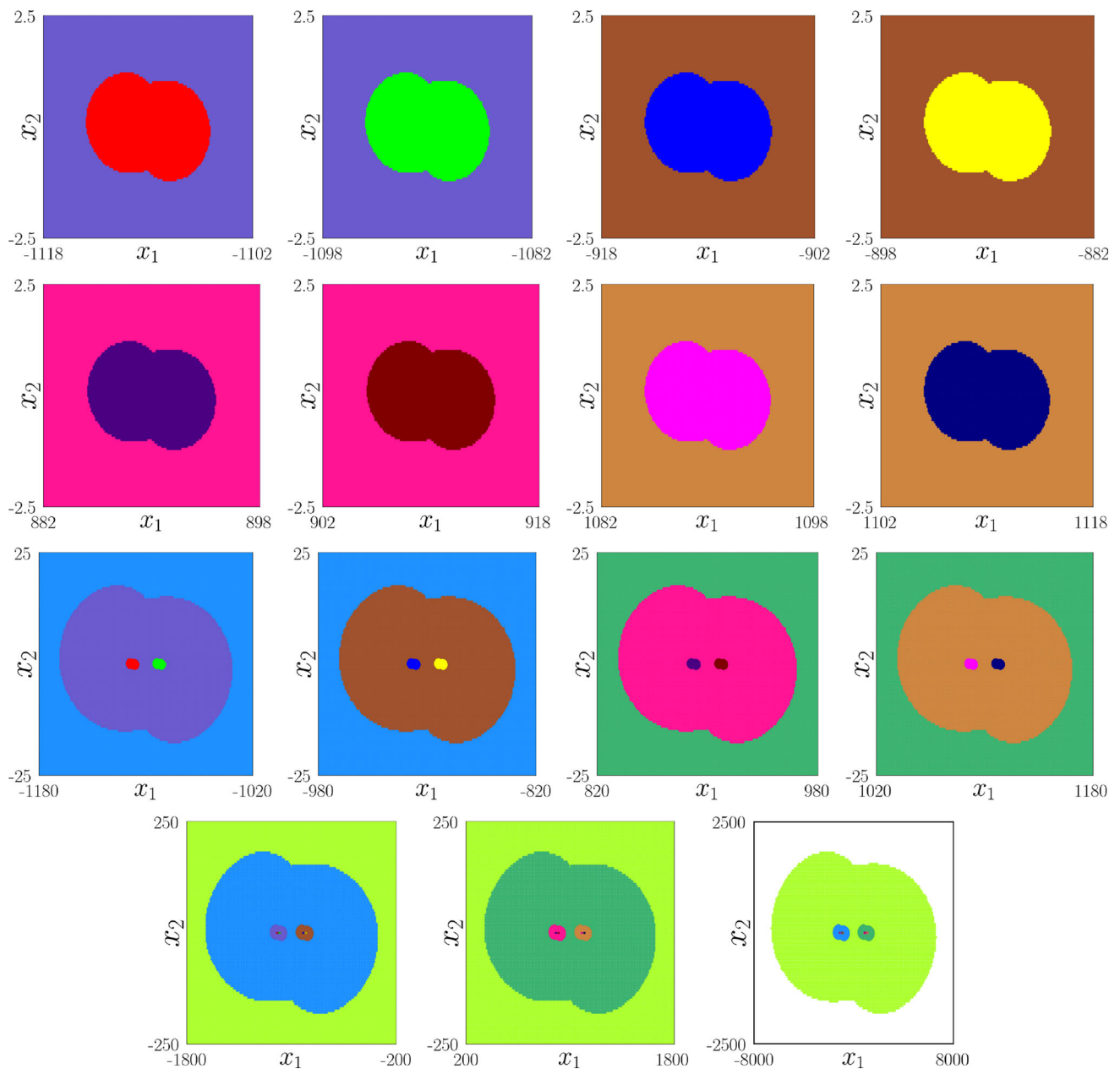
Fig. 3 Approximation of the basins of attraction of the fifteen attractors produced by the proposed construction given by (1), (2), (3) and (4) with $a = 0.2$, $b = 5$, $c = -3$, $m = 3$, $\alpha = 1$ and $\gamma = 10$ on the plane $\{\mathbf{x} \in \mathbb{R}^3 : x_3 = 0\}$, the white region is not part of any basin of attraction and a different color is assigned to each basin of attraction

References

1. G. Leonov, N. Kuznetsov, V. Vagaitsev, Phys. Lett. A **375**, 2230–2233 (2011)
2. X. Jin, X. Duan, H. Jin, Y. Ma, Entropy **22**, 610 (2020)
3. S. Jafari, J.C. Sprott, S. Mohammad Reza Hashemi Golpayegani, Phys. Lett. A **377**, 699–702 (2013)
4. D. Cafagna, G. Grassi, Commun. Nonlinear Sci. Numer. Simul. **19**, 2919–2927 (2014)
5. Z. Wang, S. Cang, E. Oketch Ochola, Y. Sun, Nonlinear Dyn. **69**, 531–537 (2012)
6. C. Li, J.C. Sprott, W. Thio, H. Zhu, IEEE Trans. Circ. Syst.-Part II Express Briefs **61**, 977–981 (2014)
7. J.M. Munoz-Pacheco, E. Zambrano-Serrano, C. Volos, S. Jafari, J. Kengne, K. Rajagopal, Entropy **20**, 564 (2018)
8. H. Xiaoyu, C. Liu, L. Liu, J. Ni, S. Li, Nonlinear Dyn. **86**, 1725–1734 (2016)

Eur. Phys. J. Spec. Top. (2022) 231:351–357

357

9. H. Xiaoyu, C. Liu, L. Liu, Y. Yao, G. Zheng, Chin. Phys. B **26**, 110502 (2017)
10. F. Rahma Tahir, S. Jafari, V.-T. Pham, C. Volos, X. Wang, Int. J. Bifurc. Chaos **25**, 1550056 (2015)
11. M.A. Kiseleva, N.V. Kuznetsov, G.A. Leonov, IFAC-PapersOnLine. In: 6th IFAC Workshop on Periodic Control Systems PSYCO 2016, **49**, 51 – 55 (2016)
12. M.-F. Danca, N. Kuznetsov, G. Chen, Nonlinear Dyn. **88**, 791–805 (2017)
13. R.J. Escalante-González, E. Campos-Cantón, Int. J. Mod. Phys. C **28**, 1750008 (2017)
14. R.J. Escalante-González, E. Campos-Cantón, M. Nicol, Chaos Interdiscipl. J. Nonlinear Sci. **27**, 053109 (2017)
15. R.J. Escalante-González, E. Campos-Cantón, IEEE Trans. Circ. Syst. II Express Briefs **66**, 1456–1460 (2019)
16. L.J. Ontañón-García, E. Campos-Cantón, Nonlinear Anal. Hybrid Syst. **26**, 38–47 (2017)
17. R.J. Escalante-González, E. Campos, Complexity **2020**, 1–12 (2020)
18. A. Wolf, J.B. Swift, H.L. Swinney, J.A. Vastano, Phys. D **16**, 285–317 (1985)
19. F. William, *Introduction to Real Analysis* (Faculty Authored and Edited Books & CDs, San Antonio, 2013)